Title	Ab initio investigation of the structure, stability, and atmospheric distribution of molecular clusters containing H2O, CO2, and N2O
Author(s)	Lemke, KH; Seward, TM
Citation	Journal of Geophysical Research, 2008, v. 113 n. 19, article no. D19304
Issued Date	2008
URL	http://hdl.handle.net/10722/58647
Rights	Journal of Geophysical Research. Copyright © American Geophysical Union.

Ab initio investigation of the structure, stability, and atmospheric distribution of molecular clusters containing H_2O, CO_2, and N_2O

Kono H. Lemke[1,2] and Terry M. Seward[1]

Received 10 July 2007; revised 12 October 2007; accepted 5 February 2008; published 9 October 2008.

[1] We present results from ab initio calculations for the structures and energetic properties of neutral clusters containing water, carbon dioxide, and nitrous oxide using the complete basis set CBS-Q multilevel procedure. Gas phase hydration energies ΔG^0, enthalpies ΔH^0, and entropies ΔS^0 for the stepwise attachment of water onto clusters according to $X\cdot(H_2O)_n + H_2O \leftrightarrow X\cdot(H_2O)_{n+1}$ ($X = CO_2$, N_2O, and H_2O) are reported for $n \leq 4$. In particular, our results demonstrate that values for the incremental hydration enthalpies and entropies of all three gases CO_2, N_2O, and H_2O asymptotically approach values characteristic of bulk water (i.e., -44.0 kJ mol^{-1} for the enthalpy and -118.8 J K^{-1} mol^{-1} for the entropy of condensation) following attachment of around three to four water molecules. Our ab initio calculations indicate that water attachment onto CO_2, N_2O, and H_2O is a thermodynamically favorable process, such that hydrated $CO_2\cdot(H_2O)_n$, $N_2O\cdot(H_2O)_n$, and $H_2O\cdot(H_2O)_n$ clusters would form a significant atmospheric repository of these species.

Citation: Lemke, K. H., and T. M. Seward (2008), Ab initio investigation of the structure, stability, and atmospheric distribution of molecular clusters containing H_2O, CO_2, and N_2O, *J. Geophys. Res.*, *113*, D19304, doi:10.1029/2007JD009148.

1. Introduction

[2] Water molecules participate in a wide variety of hydrogen and van der Waals bonds with solvent molecules to form weakly bound gas-phase moieties, i.e., water clusters [*Liu et al.*, 1996; *Keutsch and Saykally*, 2001]. Interest in the energetic and structural properties of these water clusters has increased considerably since the first spectroscopic observation of the water dimer [*Gebbie et al.*, 1969], the pioneering computational studies of Slanina and coworkers on the stability of water dimers in planetary atmospheres [*Slanina*, 1988; *Slanina et al.*, 2001, 2006, and references therein], and its implication as a causal or contributing factor in atmospheric heating [*Vaida et al.*, 2001; *Pfeilsticker et al.*, 2003; *Vaida et al.*, 2003; *Lotter*, 2006]. In order to better understand the nature and stability of water clusters, substantial efforts have been made to understand how changes in cluster structures affect their physicochemical properties and shifts in absorption spectra [*Vaida et al.*, 2001; *Kjaergaard et al.*, 2003]. Thus, in order to accurately calculate changes in energetic properties upon complexation, it is important to have an accurate description of the geometry of the complex. Furthermore, to assess the impact of clusters on the environment, the clustering equilibria and atmospheric distribution must be accurately known.

[3] Obtaining structural information as well as energetic properties of small neutral water clusters has been the focus of a number of experimental [*Curtiss et al.*, 1978, 1979; *Liu et al.*, 1996, and references therein] and a large number of theoretical studies [e.g., *Fellers et al.*, 1999; *Goldman et al.*, 2001; *Dunn et al.*, 2004; *Day et al.*, 2005; *Scribano et al.*, 2006, and references therein]. Given the importance of atmospheric water clustering reactions and the ubiquitous nature of nitrous oxide (N_2O) and carbon dioxide in the atmosphere, it should be informative to investigate the incremental attachment of solvent water onto these molecules according to simple reactions of the type,

$$X\cdot(H_2O)_n + H_2O \rightarrow X\cdot(H_2O)_{n+1} \quad (1)$$

where X represents CO_2 and N_2O and to determine the corresponding energetic trends of solvation, cluster structures as well as atmospheric abundances.

[4] Structural information on small carbon dioxide water clusters (i.e., $n = 1-2$) have been previously obtained from microwave spectroscopic experiments on the $CO_2\cdot H_2O$ [*Peterson and Klemperer*, 1984] and $CO_2\cdot(H_2O)_2$ clusters [*Peterson et al.*, 1991] as well as from ab initio studies on the $CO_2\cdot(H_2O)_2$ [*Nguyen and Ha*, 1984] and $CO_2\cdot(H_2O)_{3-4}$ clusters [*Nguyen et al.*, 1997]. These studies demonstrated that (1) a T-shaped complex would be the dominant $CO_2\cdot(H_2O)$ structure, (2) the $CO_2\cdot(H_2O)_2$ structure was found to be cyclical with one water molecule oxygen-bound to the carbon atom and the second water molecule hydrogen bonded to one of the CO_2 oxygens, and (3) the higher clusters, $CO_2\cdot(H_2O)_{3-4}$, would have typical cyclic structures where the CO_2 molecule folds onto the H_2O-ring edge.

[1] Institute of Mineralogy and Petrology, ETH Zurich, Zurich, Switzerland.
[2] Now at Department of Earth Sciences, University of Hong Kong, Hong Kong.

0148-0227/08/2007JD009148

[5] There are significantly fewer studies concerning water clustering onto nitrous oxide and these efforts have centered chiefly on the first hydration step which results in the formation of $N_2O{\cdot}H_2O$. Particularly noteworthy is the study by *Zolandz et al.* [1992] who performed microwave spectroscopic/mass spectrometric experiments on the $N_2O{\cdot}H_2O$ cluster. Their study demonstrated that a tilted, T-shaped $N_2O{\cdot}H_2O$ structure having a typical second hydrogen bond within the complex is probably the most valid cluster configuration. More recent results of a combined IR and ab initio study of the $N_2O{\cdot}H_2O$ cluster by *Wójcik et al.* [2001] as well as results from a high-resolution IR study by *Gimmler and Havenith* [2002] provide support for the predominance of a planar tilted $N_2O{\cdot}H_2O$ geometry. There are apparently no reported experimental or quantum chemical data on the geometries for $N_2O{\cdot}(H_2O)_n$ clusters with $n > 1$.

[6] The situation for small $H_2O{\cdot}(H_2O)_n$ clusters is quite different. Water clusters have been studied extensively both by experiment and theoretically to gain insight into their structures as well as energetic properties and have been shown to be planar with substantial binding energies. For instance, $H_2O{\cdot}(H_2O)_2$, $H_2O{\cdot}(H_2O)_3$, and $H_2O{\cdot}(H_2O)_4$ have characteristic cyclic structures and are characterized by significant hydrogen bonding (e.g., the binding energy of $H_2O{\cdot}H_2O$ is around 8.2 kJ mol^{-1} [*Curtiss et al.*, 1979]). Note that information of structural and energetic properties of higher $X{\cdot}(H_2O)_n$ clusters ($n \leq 4$) is relatively limited, especially for N_2O and CO_2 hydrates, and thus further work on the subject is required. Clearly, the solvation of N_2O, CO_2, and H_2O by more than one water molecule, for instance, for $n \leq 4$, plays an important role in our understanding of large weakly bound van der Waals type clusters, but it can also yield insight into the solubility of these gases into larger clusters, aerosols, water droplets, and bulk liquid water as well as provide fundamental molecular-scale information into the size, stability, and atmospheric distribution of these greenhouse agents.

[7] In this report, we have used high-accuracy ab initio complete basis set CBS-Q theory [*Ochterski et al.*, 1996] to calculate structures, energetic trends of salvation, and atmospheric abundances of the $N_2O{\cdot}(H_2O)_n$, $CO_2{\cdot}(H_2O)_n$, and $H_2O{\cdot}(H_2O)_n$ clusters. In detail, we report both stepwise and total hydration free energies, enthalpies, and entropies for the lowest energy isomers for $N_2O{\cdot}(H_2O)_n$ ($n \leq 5$), $CO_2{\cdot}(H_2O)_n$ ($n \leq 5$), and $H_2O{\cdot}(H_2O)_n$ ($n \leq 4$) as well as results for the pressure and number density of each greenhouse hydrate in atmospheric media up to 45 km altitude.

2. Computational Methods

[8] Quantum chemical calculations for the clusters $N_2O{\cdot}(H_2O)_n$, $CO_2{\cdot}(H_2O)_n$, and $H_2O{\cdot}(H_2O)_n$ were carried out using the multilevel CBS-Q [*Ochterski et al.*, 1996], CBS-QCI/APNO [*Montgomery et al.*, 1994], and G3 [*Curtiss et al.*, 1998] model chemistry as implemented in the GAUSSIAN03 package [*Frisch et al.*, 2003]. The general approach in the above methods is to first determine the structure and zero point energy of a molecule at a low level of theory (i.e., HF/6−31G) and then perform higher-level single point calculations on a higher-accuracy geometry using larger basis set In detail, the CBS-Q method builds on a sequence (six steps) of calculations at the CCISD(T), MP4(SDQ), MP2 (with complete basis set extrapolation), and HF (first geometry and frequency determination) level with increasingly larger basis sets. The largest basis set used in the CBS-Q method is the 6−311++G(3*d*2*f*,2*df*,2*p*) where the values in parenthesis indicate the multiple sets of polarization functions used for the second row elements, first row elements, and hydrogen, respectively.

[9] The CBS-Q procedure, as has been pointed out previously [*Ochterski et al.*, 1996] yields reliable geometries and frequencies, necessary for accurate energy calculations. For instance, the mean absolute deviation of the CBS-Q method from experiment for 125 energies in the G2/97 test set [*Curtiss et al.*, 2000] is 4.1 kJ mol^{-1} and therefore within the range of chemical accuracy (i.e., ±4.18 kJ mol^{-1}). It should be mentioned that the CBS-Q method does not suffer from basis set superposition errors (i.e., the CBS-Q method is by definition BSSE-free and thus does not require counterpoise-type procedures to correct for basis set truncation). It should also be noted that the theoretical binding energies of hydrogen bonded clusters without BSSE corrections often more closely reproduce experimental clustering equilibria as BSSE and basis set truncation errors cancel (see *Dunning* [2000] and *Masamura* [2001] for a review on BSSE correction procedures and cluster binding energies). In addition, given the relatively small contribution of vibrational anharmonicity to the binding energies in small water clusters as demonstrated by *Diri et al.* [2005] (e.g., anharmonicity corrections to theoretical binding energies of $(H_2O)_6$ are less than 4 kJ mol^{-1}), we have not introduced such corrections into the results of the CBS-Q calculations. However, one of the key deficiencies in CBS-Q theory is that basis set expansion and increasing the degree of correlation contributes significantly to the cost of the calculation. Consequently, CBS-Q type calculations on clusters are currently limited to around eight water molecules [*Likholyot et al.*, 2007].

3. Calculation of Atmospheric Cluster Abundances

[10] In order to link the computational results from this study with atmospheric composition and chemistry, we have calculated the temperature-dependent changes in the free energies of the clustering reactions, ΔG^o, for $N_2O{\cdot}(H_2O)_n$, $CO_2{\cdot}(H_2O)_n$, and $H_2O{\cdot}(H_2O)_n$ formation according to equation (1). Values for the free energies have been calculated from the CBS-Q data including the thermal corrections for the specified temperature. The CBS-Q procedure initially yields the zero-point-corrected electronic energy E_O (at zero Kelvin), which is obtained from the zero-point energy (ZPE) and electronic energy ($E_{Elec.}$) according to the relationship

$$E_O = E_{Elec.} + ZPE \tag{2}$$

The value for E_O is then used to compute the thermally corrected energy, E, and enthalpy, $H_{Therm.}$, according to

$$E = E_O + E_{Trans} + E_{Rot} + E_{Vib} \tag{3}$$

and

$$H_{Therm.} = E + RT \tag{4}$$

where E_{Trans}, E_{Rot}, E_{Vib} represent the translational, rotational, and vibrational contributions to the energy and R is the gas constant. The free energy is then obtained from the well-known relationship

$$\Delta G^o = \Delta H^o - T\Delta S^o \tag{5}$$

and is easily transformed to yield the equilibrium constant, K, for the cluster forming reaction (1) according to

$$K = \exp(-\Delta G^o/RT) \tag{6}$$

where ΔG^o represents the standard free energy change for the cluster forming reaction (1). Values of the equilibrium constants are then applied together with reported values for the atmospheric pressures of H_2O, and X (X = CO_2 or N_2O) to yield values for the atmospheric pressure of the cluster $X{\cdot}(H_2O)_n$ as in

$$P_{X\cdot(H_2O)_n} = K_{X\cdot(H_2O)_n} \cdot P^n_{H_2O} \cdot P_X \tag{7}$$

where $P_{X\cdot(H_2O)_n}$ is the partial pressure of the cluster, $K_{X\cdot(H_2O)_n}$ is the equilibrium constant for the clustering reaction, $P^n_{(H_2O)}$ is the water vapor pressure, and P_X is the solute partial pressure (i.e., P_{CO_2} and P_{N_2O}). Applying calculated values for $K_{X\cdot(H_2O)_n}$ and reported data for P_{H_2O}, P_{N_2O}, and P_{CO_2} [*Brasseur and Solomon*, 2005], we are able to generate pressure and number density profiles for water cluster as a function of atmospheric altitude.

4. Results and Discussions

[11] We begin our discussion by comparing results for cluster structures of our ab initio calculations with those obtained from select spectroscopic methods. We then briefly discuss recent experimental and theoretical efforts aimed at quantifying water dimerization equilibrium constants as well as to compare our current results with those measured previously. In the final section, we present results of calculations of the atmospheric abundances of molecular clusters with up to five water molecules.

4.1. Structures

[12] The MP2/6−31(d) optimized structures and key geometric parameters for the $N_2O{\cdot}(H_2O)_n$, $CO_2{\cdot}(H_2O)_n$, and $H_2O{\cdot}(H_2O)_n$ clusters are shown in Figure 1. Table 1 lists CBS-Q calculated and experimental geometric parameters as well as binding energies, when available, for the monohydrates $N_2O{\cdot}(H_2O)$, $CO_2{\cdot}(H_2O)$, and $H_2O{\cdot}(H_2O)$. Structural data for the monohydrates have been obtained from microwave spectroscopic studies; however, we are not aware of any experimental studies which report geometries for the $N_2O{\cdot}(H_2O)_2$, $N_2O{\cdot}(H_2O)_3$, $CO_2{\cdot}(H_2O)_3$ and higher carbon dioxide water clusters.

[13] As can be seen from Figure 1, we identified one principal monohydrate $N_2O{\cdot}(H_2O)$ cluster, namely the bent T-shaped structure **a1**, hich a second weak bond is

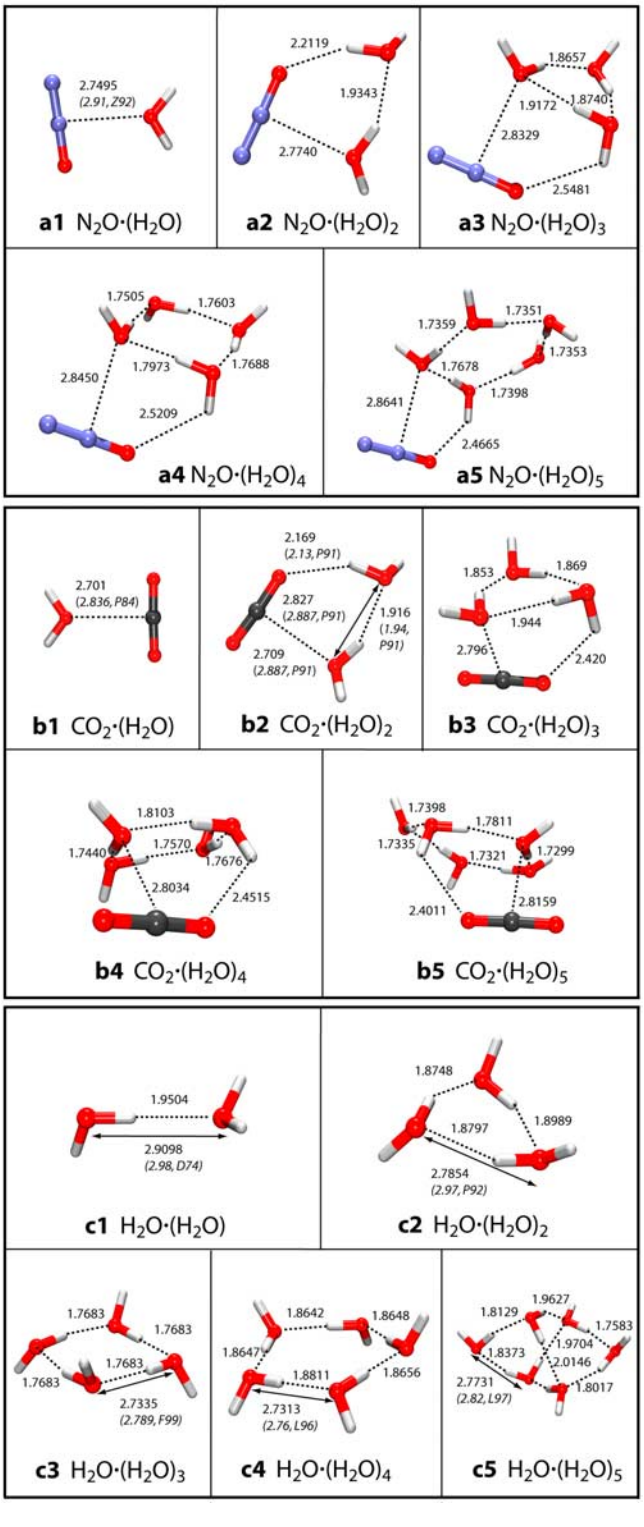

Figure 1. MP2/6−31G(d) optimized geometries for neutral water clusters containing H_2O, CO_2, and N_2O (Z92 [*Zolandz et al.*, 1992], P84 [*Peterson and Klemperer*, 1984], P91 [*Peterson et al.*, 1991], D74 [*Dyke and Muentner*, 1974], P92 [*Pugliano and Saykally*, 1992], F99 [*Fellers et al.*, 1999], L96 [*Liu et al.*, 1996], L97 [*Liu et al.*, 1997b]).

Table 1. Comparison Between Theoretical and Experimental Clustering Energies and Relevant Geometric Parameters

	ΔG^0 (kJ mol^{-1})		$R_{X\cdots O}$ (Å)	
	Calc.	Exp.	Calc.	Exp.
$H_2O{\cdot}H_2O$	7.5[a]	8.2 ± 2.7[d]	2.909[a]	2.98[e]
	8.6[b]		2.925[b]	
	8.3[c]		2.914[c]	
$CO_2{\cdot}H_2O$	12.7[a]	12.3[f]	2.710[a]	2.84[g]
$N_2O{\cdot}H_2O$	15.4[a]	-	2.749[a]	2.91[h]

[a]CBS-Q.
[b]CBS-QCI/APNO.
[c]G3.
[d]*Curtiss et al.* [1979].
[e]*Dyke and Muentner* [1974].
[f]*Coan and King* [1971].
[g]*Peterson and Klemperer* [1984].
[h]*Zolandz et al.* [1992].

formed between a hydrogen on water and the oxygen on N_2O. Given that the bent T-shaped geometry has previously been identified in the microwave spectroscopic work on $N_2O{\cdot}(H_2O)$ by *Zolandz et al.* [1992], isomer **a1** was taken as the basis for all subsequent energy, frequency, and atmospheric abundance calculations. For the other monohydrates, $H_2O{\cdot}(H_2O)$ and $CO_2{\cdot}(H_2O)$, the agreement between the CBS-Q values for the reaction free energies and experimentally determined energies is good (see Table 1). There are only minor discrepancies between calculated CBS-Q and experimentally observed geometries for all three monohydrates. The largest discrepancy was found for the $R_{N\cdots O}$ distance in the $N_2O{\cdot}(H_2O)$ cluster, where the calculated distance is larger by 0.16Å than the reported microwave measurement of *Zolandz et al.* [1992]. Interestingly, our calculated CBS-Q estimate for the intermolecular oxygen (water) – nitrogen (nitrous oxide) bond distance of 2.749Å (see Table 1) agrees very well with other ab initio bond distances, i.e., the MP2/6−31++G** theory level work by *Wójcik et al.* [2001] which yielded a 2.798Å distance and the BSSE corrected MP2 study reported by *Cox et al.* [1994] (2.776Å).

[14] There are no reported experimental data for the structures and binding energies of the $N_2O{\cdot}(H_2O)_n$ series for n > 1 and of the $CO_2{\cdot}(H_2O)_n$ series for n > 2, except for one microwave study by *Peterson et al.* [1991], where the authors reported the structure of the $CO_2{\cdot}(H_2O)_2$ cluster. As may be seen from Figure 1, the CBS-Q calculated geometric parameters for the $CO_2{\cdot}(H_2O)_2$ cluster **b2** agree well with the values provided by *Peterson et al.* [1991]; however, it is noted, as for the $CO_2{\cdot}(H_2O)$ cluster (**b1**, Figure 1), that the calculated $R_{C\cdots O}$ distance in the $CO_2{\cdot}(H_2O)_2$ cluster is around 0.18Å shorter than the measured value of 2.877Å.

4.2. Clustering Thermochemistry

[15] The next section deals with the energetics of water attachment onto H_2O, N_2O, and CO_2 but will be proceeded by a brief discussion on the energetic trends of water dimerization. The motivation here is to test our methods for calculating energetic properties of the water dimer and compare our computed values with available experimental values. Figure 2 represents the CBS-Q, G3, and CBS-QCI/APNO calculated water dimerization equilibrium constants for the temperature range 290−420 K. Also shown are experimental results at elevated temperatures (357−383 K) obtained from thermal conductivity measurements by *Curtiss et al.* [1979], direct measurement of the dimer concentration by *Pfeilsticker et al.* [2003] (292.4 K), *Ptashnik et al.* [2004] (292 and 342 K), and *Lotter* [2006] (301 K) by atmospheric long path visible and near-IR absorption spectroscopy as well as the more recent results from VRT potential calculations by *Scribano et al.* [2006].

[16] From Table 1 and Figure 2, it can be seen that all three ab initio methods, CBS-Q, and especially CBS-QCI/APNO and G3, yield values for the free energy of water dimerization (or equilibrium constant $\ln K_p$) that are in excellent agreement with the thermal conductivity measurements of *Curtiss et al.* [1979] obtained in the range 357−383 K. In addition, G3 and CBS-QCI/APNO perform somewhat better than CBS-Q theory. However, theoretical values for the water dimerization energy (or $\ln K_p$)

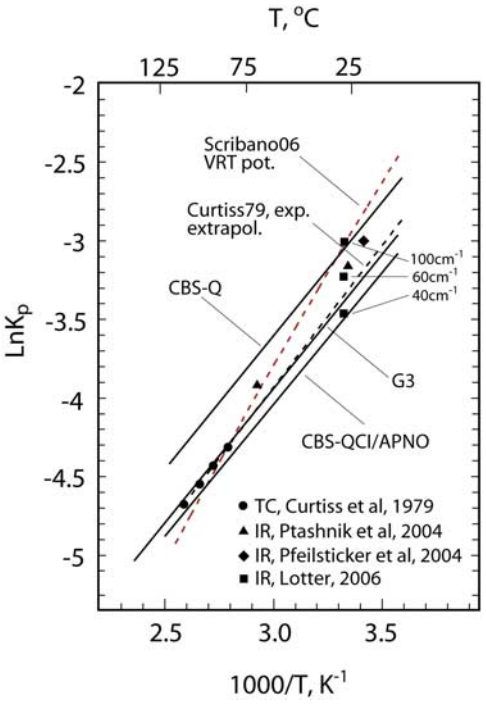

Figure 2. Van't Hoff diagram for the water dimer system. Symbols represent reported measurements for the water dimerization ($2H_2O = H_2O{\cdot}H_2O$) equilibrium constant $\ln K_p$, dashed lines are extrapolated experimental [*Curtiss et al.*, 1979] ($\Delta H^0 = -15.0 \pm 2.1$ kJ mol^{-1} and $\Delta S^o = -77.8 \pm 5.4$ J · K^{-1} mol^{-1}) and VRT potential data [*Scribano et al.*, 2006]. Quantum chemical values for the dimerization constant reported in this study are shown as solid lines and have been calculated at CBS-Q ($\Delta H^0 = -14.4$ kJ mol^{-1} and $\Delta S^0 = -73.7$ J K^{-1} mol^{-1}), CBS-QCI/APNO ($\Delta H^0 = -14.5$ kJ mol^{-1} and $\Delta S^0 = -77.0$ J K^{-1} mol^{-1}) and G3 ($\Delta H^0 = -14.4$ kJ mol^{-1} and $\Delta S^0 = -76.9$ J K^{-1} mol^{-1}) theory level (values of ΔH^0 and ΔS^0 refer to water dimerization enthalpy and entropy changes). Equilibrium constants obtained from IR-measurements reported by *Lotter* [2006] are shown for three water dimer FWHM values, 40, 60, and 100 cm^{-1}.

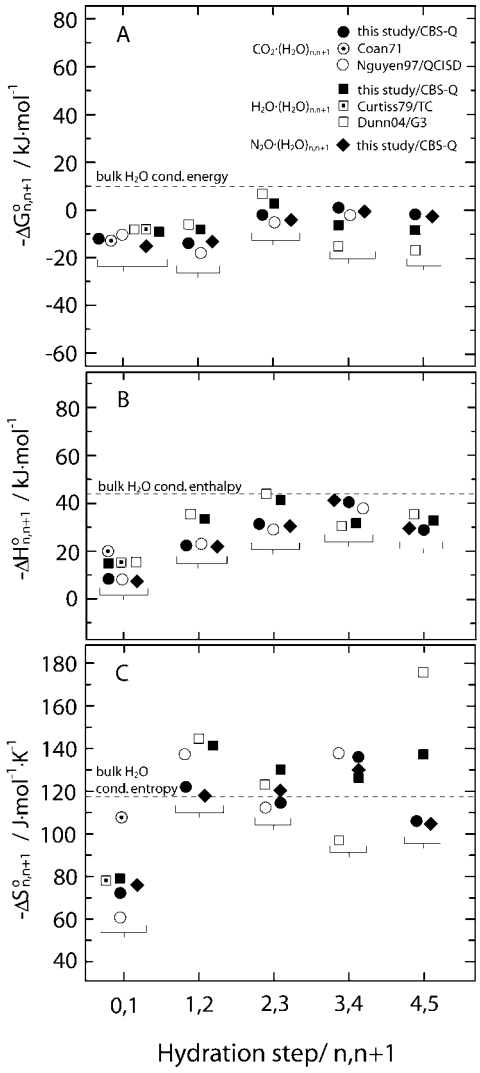

Figure 3. Comparison of experimental and quantum chemical (a) free energy, (b) enthalpy, and (c) entropy changes for H_2O, CO_2, and N_2O hydration at 298 K and 1 bar. Also shown are reported energetic data from ab initio studies by *Nguyen et al.* [1997] for CO_2 hydration and *Dunn et al.* [2004] for water clusters.

obtained by all three methods are within the reported experimental error limits (see Table 1 and *Curtiss et al.* [1979]) (due to the very high computational cost involved, we did not apply the G3 and CBS-QCI/APNO methods to larger hydrates (i.e., $n > 1$); instead, for reasons of consistency we have used the CBS-Q method for all calculations of clusters with $n > 1$). Also displayed are the extrapolated values of $\ln K_p$, which are based on van't Hoff analysis of enthalpy and entropy changes ($\Delta H^0 = -15.0 \pm 2.1$ kJ mol^{-1} and $\Delta S^0 = -77.8 \pm 5.4$ J K^{-1} mol^{-1}) for the water dimerization reaction as reported by *Curtiss et al.* [1979] assuming isothermicity of ΔH^0 and ΔS^0. It is worth noting that there have been several theoretical studies suggesting that ΔH^0 and ΔS^0 vary significantly over temperature [*Scribano et al.*, 2006]. However, given the paucity of reliable experimental data for the water dimerization equilibrium constant, we focus on the energetic trends reported by *Curtiss et al.* [1979] and adopt the approach applied in previous theoretical studies [*Dunn et al.*, 2004], in which ΔH^0 and ΔS^0 are taken to be temperature-independent. Also, as may be seen from Figure 2, there are considerable differences between reported values of $\ln K_p$, at the same temperature (i.e., 300 K), and those obtained by *Curtiss et al.* [1979]. It appears that results of near-IR measurements of atmospheric water vapor [*Pfeilsticker et al.*, 2003; *Ptashnik et al.*, 2004; *Lotter*, 2006] provide a less accurate estimate of the dimerization constant and values of $\ln K_p$ obtained by vibrational spectroscopy should therefore be treated with some caution. Interestingly, in a recent report by *Lotter* [2006], the author noted that results from near-IR atmospheric measurements of the water dimer by *Pfeilsticker et al.* [2003] had to be revoked, as their findings could not be confirmed by subsequent measurements.

[17] Energetic trends of hydration in the $H_2O\cdot(H_2O)_n$, $N_2O\cdot(H_2O)_n$, and $CO_2\cdot(H_2O)_n$ cluster series are shown in Figures 3a, 3b, and 3c for the incremental attachment of water onto H_2O, N_2O, and CO_2 at 298 K and 1 bar. As may be seen from Figure 3, CBS-Q free energy and enthalpy (and thus entropy) changes for the formation of the H_2O and CO_2 monohydrates from constituent monomers (equation (1), $n = 0$) are in good agreement with experimental values reported by *Curtiss et al.* [1979] (for $H_2O\cdot H_2O$) and *Coan and King* [1971] (for $CO_2\cdot H_2O$). For example, the CBS-Q free energy changes for $H_2O\cdot H_2O$ and $CO_2\cdot H_2O$ formation from constituent monomers differ from experiment by only 0.7 and 0.4 kJ mol^{-1}, respectively (Table 1 and Figure 3). Unfortunately, there are no experimental data for the hydration energy of N_2O to the monohydrate $N_2O\cdot H_2O$.

[18] Figure 3 also shows CBS-Q theoretical values for ΔG^0, ΔH^0, and ΔS^0 for the hydration of carbon dioxide with up to five water molecules. Interestingly, the CBS-Q computed values of ΔG^0 for CO_2 hydration asymptotically approach, from below (i.e., from more endergonic values), the bulk water condensation value of -8.8 kJ mol^{-1} [*Linstrom and Mallard*, 2005]. The same trend can also be observed for the hydration enthalpy of CO_2 (bulk hydration enthalpy -44.0 kJ mol^{-1}), whereas incremental values for the entropies oscillate around the bulk limit value (-118.1 J K^{-1} mol^{-1}), which is not unexpected, given that values of ΔS^0 are particularly sensitive to changes in cluster configuration. However, values of ΔG^0, ΔH^0, and ΔS^0

Table 2. Calculated CBS-Q Total Energies for Nitrous Oxide Hydration as a Function of Temperature

		ΔG^0_{total} (kJ mol^{-1})		
T (K)	Altitude (km)	$N_2O\cdot H_2O$	$N_2O\cdot(H_2O)_2$	$N_2O\cdot(H_2O)_3$
298.2	0	15.4	28.3	33.1
250.2	5	11.6	18.9	17.9
215.6	10	8.9	11.9	6.7
198.0	15	7.5	8.4	1.0
208.0	20	8.3	10.4	4.3
216.1	25	8.9	12.0	6.9
221.5	30	9.4	13.1	8.6
228.1	35	9.9	14.4	10.8
240.5	40	10.9	16.9	14.7
251.9	45	11.8	19.2	18.4

Table 3. Calculated CBS-Q Total Energies for Carbon Dioxide Hydration as a Function of Temperature

		ΔG^0_{total} (kJ mol^{-1})			
T (K)	Altitude (km)	$CO_2 \cdot H_2O$	$CO_2 \cdot (H_2O)_2$	$CO_2 \cdot (H_2O)_3$	$CO_2 \cdot (H_2O)_4$
298.2	0	12.7	26.6	32.9	29.9
250.2	5	5.3	13.2	13.5	4.5
215.6	10	4.2	7.6	3.7	−9.8
198.0	15	3.5	4.8	−1.3	−17.0
208.0	20	3.9	4.3	−0.6	−15.1
216.1	25	4.2	7.7	3.8	−9.6
221.5	30	4.4	8.6	5.3	−7.4
228.1	35	4.6	9.6	7.2	−4.7
240.5	40	5.0	11.6	10.7	0.4
251.9	45	5.4	13.4	13.9	5.1

appear to converge toward bulk condensation values (dashed lines shown in Figure 3) with increasing cluster size, which suggests that the thermochemical properties of water in clusters containing three to four water molecules do not differ significantly from the properties of water in larger clusters, aerosols, water droplets, or even bulk liquid water.

[19] It should be noted that the low-energy equilibrium structures of the $CO_2 \cdot (H_2O)_n$ clusters reported here (see Figure 1) differ substantially from ab initio structures reported by *Jena and Mishra* [2005]. For example, their $CO_2 \cdot (H_2O)_3$ and $CO_2 \cdot (H_2O)_4$ clusters lie around 14.4 kJ mol^{-1} and 16.7 kJ mol^{-1}, respectively, higher than the **b3** and **b4** isomers reported here. It is therefore likely that $CO_2 \cdot (H_2O)_n$ clusters (for $n > 2$) reported by *Jena and Mishra* [2005] represent local minima and do not represent true global minimum structures. In contrast, CBS-Q values for the hydration of CO_2 with up to four waters reported here are in excellent agreement with the recent values obtained at the QCISD(T)//MP2/6−31G(d,p) level by *Nguyen et al.* [1997] (see Figure 3). Theoretical CBS-Q values for ΔG^0 for the first four hydration steps of carbon dioxide are all within 2−3 kJ mol^{-1} of the ab initio results by *Nguyen et al.* [1997]. Finally, we are not aware of any experimental determinations of hydration equilibria in higher carbon dioxide water clusters ($n > 1$). However, given the excellent agreement between the CBS-Q cluster geometry reported here and microwave data for the monohydrate and dihydrate as well as high-level ab initio energies and geometries for the higher $CO_2 \cdot (H_2O)_n$ clusters [*Nguyen et al.*, 1997], we are confident that the CBS-Q level $CO_2 \cdot (H_2O)_n$ clustering equilibria reported here represent a new and accurate data set.

[20] The calculated energetic trends for N_2O hydrates are similar to those of the $CO_2 \cdot (H_2O)_n$ clusters (see Figure 3). In particular, the enthalpies for N_2O hydration follow those closely of CO_2, (i.e., values for the stepwise hydration ΔH^0 for N_2O are within less than 1 kJ mol^{-1} of the same reaction with CO_2 up to clusters with five water molecules and similarly converge toward bulk limits). As in the case of the $CO_2 \cdot (H_2O)_n$ cluster series, the stepwise attachment of H_2O onto $N_2O \cdot (H_2O)$ is likely to be dominated by the formation of ring-type structures (Figure 1a). Formation of the $N_2O \cdot (H_2O)$, $N_2O \cdot (H_2O)_2$, $N_2O \cdot (H_2O)_3$, $N_2O \cdot (H_2O)_4$, and $N_2O \cdot (H_2O)_5$ releases around 15.4, 12.9, 4.8, −2.7, and 2.1 kJ mol^{-1} per H_2O molecule, respectively. Unfortunately, there are no experimental data for water clustering onto $N_2O \cdot (H_2O)_n$; however, just as for the $CO_2 \cdot H_2O$ cluster, there is good agreement between the theoretical CBS-Q and the experimental microwave geometry for $N_2O \cdot H_2O$ [*Zolandz et al.*, 1992], which, in turn, lends support to the accuracy of the clustering thermochemistry reported here. Also shown in Figure 3 are the CBS-Q values for ΔG^0, ΔH^0, and ΔS^0 for water clustering up to the hexamer cage. The corresponding water cluster structures are depicted in Figure 1. Water cluster geometries as well as their corresponding energetic properties have been studied in detail previously by experiment [*Liu et al.*, 1994; *Cruzan et al.*, 1996; *Liu et al.*, 1997a, 1997b] and by ab initio methods [*Dunn et al.*, 2004; *Day et al.*, 2005]. The reader is referred to these reports and references therein for a detailed description of small water clusters.

4.3. Atmospheric Cluster Distribution

[21] The thermodynamic data employed to calculate individual clustering equilibria and cluster abundances in the

Table 4. Calculated CBS-Q Total Energies for Water Hydration as a Function of Temperature

		ΔG^0_{total} (kJ mol^{-1})			
T (K)	Altitude (km)	$H_2O \cdot H_2O$	$H_2O \cdot (H_2O)_2$	$H_2O \cdot (H_2O)_3$	$H_2O \cdot (H_2O)_4$
298.2	0	7.5	16.8	14.1	20.7
250.2	5	5.2	6.3	−2.5	−7.0
215.6	10	2.2	−1.5	−14.9	−22.7
198.0	15	0.9	−5.4	−21.1	−30.7
208.0	20	1.7	−3.2	−17.5	−26.2
216.1	25	2.4	−1.4	−14.7	−22.5
221.5	30	2.9	−0.2	−12.8	−20.1
228.1	35	3.4	1.3	−10.5	−14.2
240.5	40	4.4	4.0	−6.1	−11.5
251.9		5.3	6.6	−2.1	−6.3

atmosphere are listed in Tables 2, 3, and 4. Using reported monomer abundances [*Brasseur and Solomon*, 2005] and energetic data for individual clustering reactions from Tables 2, 3, and 4 in conjunction with equation (6) and (7), we have calculated the atmospheric abundances (i.e., partial pressures in units atm) as well as number densities (i.e., cluster molecules per cm^3) of the $N_2O\cdot(H_2O)_n$, $CO_2\cdot(H_2O)_n$, and $H_2O\cdot(H_2O)_n$ series up to 45 km altitude and results thereof are shown in Figures 4a, 4b, and 4c, respectively.

[22] As may be seen from Figures 4a, 4b, and 4c, there are significant similarities between the abundances of $N_2O\cdot(H_2O)_n$, $CO_2\cdot(H_2O)_n$, and $H_2O\cdot(H_2O)_n$ clusters. First, the abundances for all clusters decrease with increasing altitude and second, the pressure profiles for the smaller clusters (i.e., with one and two water molecules) exhibit a moderate inflection at around 15–20 km altitude. The former is easily explained by the decreasing water vapor pressure with increasing altitude and the increasing effect of the water monomer pressure on the abundance of higher hydrates (see equation (7)). Thus, although the atmospheric abundances of the monohydrate $N_2O\cdot(H_2O)$, $CO_2\cdot(H_2O)$, and $H_2O\cdot(H_2O)$ are governed by the shifting balance between changes of the clustering equilibria and monomer abundances, the abundances of larger clusters are foremost dominated by the exponential water monomer term in equation (7). The second notable feature at around 15–20 km (i.e., tropospause) arises from a distinct temperature inversion (see Figure 3) in this region of the atmosphere and the effect of this temperature change on the clustering energies is clearly seen in Tables 2, 3, and 4.

[23] The clustering energies derived from CBS-Q calculations and reported monomer partial pressures have also been applied to predict cluster number densities at each temperature and results thereof are summarized in Table 5. As can be seen from Table 5, $H_2O\cdot H_2O$ clusters represent the largest fraction of the three monohydrates up to around 10 km altitude, whereas number densities of $CO_2\cdot H_2O$ clusters are predicted to exceed those of the $N_2O\cdot H_2O$ cluster as well as water dimer in the interval from 15 to 40 km altitude. It should be noted that atmospheric pressures of $CO_2\cdot(H_2O)$ and $H_2O\cdot(H_2O)$ clusters have been previously calculated using QCSID level theory [*Kjaergaard et al.*, 2003] and these data are in very good agreement with results presented here. For instance, Kjaergaard and coworkers estimate that the 298 K sea level $H_2O\cdot H_2O$ cluster pressure is around 4×10^{-6} atm (or 9.8×10^{13} $H_2O\cdot H_2O$ molecules per cm^3), which is in the same range as the CBS-Q theory level cluster pressure and density values of around 7.6×10^{-6} atm and 1.9×10^{14} cm^{-3}, respectively, reported here. In contrast, in a recent theoretical study, *Dunn et al.* [2004] reported a substantially higher value for the water dimer pressure and density at 298 K (i.e., 3×10^{-5} atm and 1.1×10^{15} cm^{-3}), which can be attributed chiefly to their high water monomer pressure (0.031 atm versus 0.017 atm as reported by *Brasseur and Solomon* [2005]). It should be noted that minor variations in water vapor pressure can have substantial effects on the calculated dimer pressure due to the squared dependence of the equilibrium dimer pressure on P_{H_2O}.

[24] Recently, *Lotter* [2006] reported measurements of $H_2O\cdot H_2O$ absorption b ve long path differential optical absorption spectroscopy (DOAS) in atmospheric media at 301 K and provided values for the water dimerization equilibrium constants K_p (i.e., for the 747 nm water dimer band full width at half maximum, FWHM, of 40 cm^{-1} K_p =

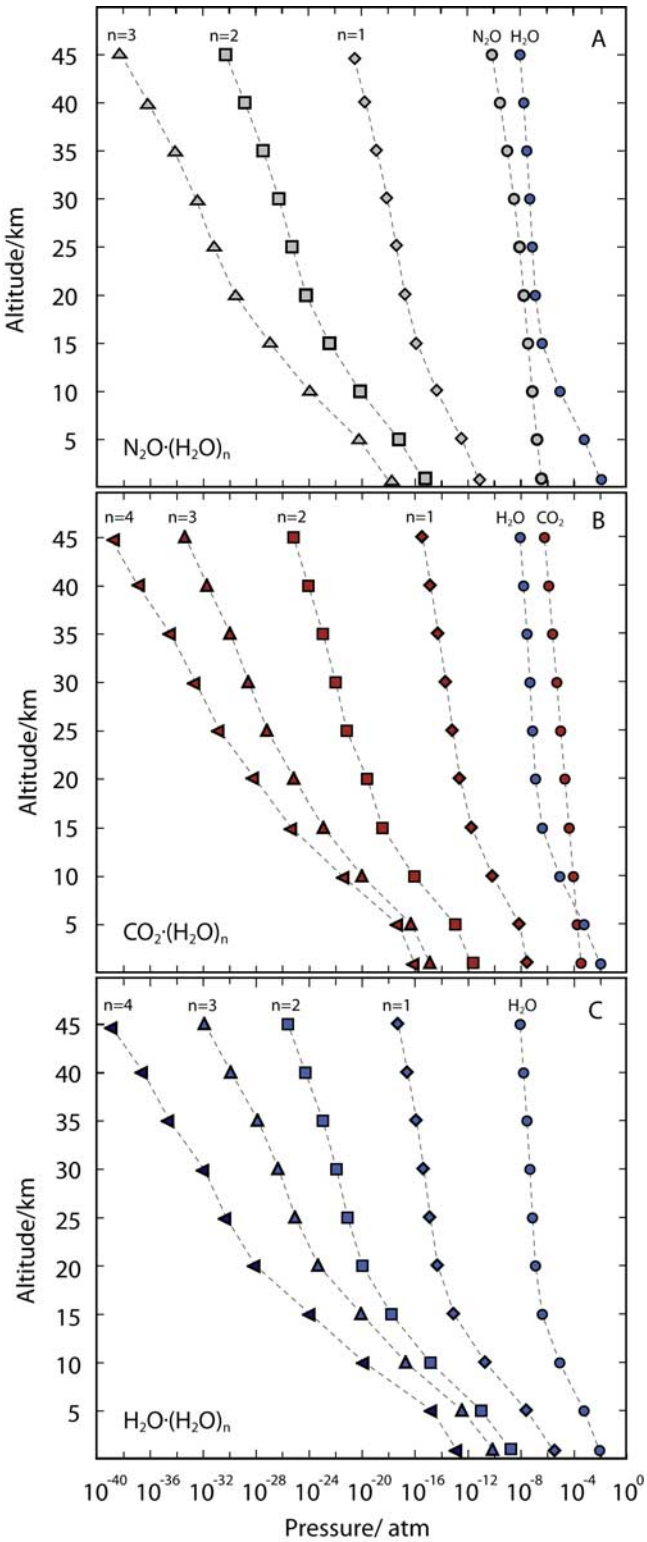

Figure 4. Atmospheric altitude profiles (≤45 km) for the partial pressures of the (a) $N_2O\cdot(H_2O)_n$, (b) $CO_2\cdot(H_2O)_n$, and (c) $H_2O\cdot(H_2O)_n$ cluster series.

Table 5. Partial Pressures and Number Densities of Molecular Clusters Calculated (CBS-Q Theory) to be Presented in the Atmosphere up to 45 km Altitude

		$P_{cluster}$ (atm), $N_{cluster}$ (cm^{-3})						
T (K)	Altitude (km)	$H_2O{\cdot}H_2O$	$H_2O{\cdot}(H_2O)_2$	$H_2O{\cdot}(H_2O)_3$	$N_2O{\cdot}(H_2O)$	$N_2O{\cdot}(H_2O)_2$	$N_2O{\cdot}(H_2O)_3$	$CO_2{\cdot}(H_2O)$	$CO_2{\cdot}(H_2O)_2$	$CO_2{\cdot}(H_2O)_3$
298.2	0	7.64×10^{-6},	5.37×10^{-9},	2.77×10^{-10},	1.11×10^{-11},	1.01×10^{-15},	2.46×10^{-18},	3.84×10^{-8},	2.41×10^{-12},	3.22×10^{-15},
		1.88×10^{14},	1.32×10^{11},	6.84×10^{9},	2.73×10^{8},	2.49×10^{4}	6.07×10^{1}	9.46×10^{11},	5.95×10^{7}	7.93×10^{4}
250.2	5	2.83×10^{-8},	9.71×10^{-12},	3.88×10^{-13},	3.41×10^{-13},	6.15×10^{-18},	1.56×10^{-21},	7.91×10^{-9},	1.11×10^{-13},	5.45×10^{-17},
		8.31×10^{11},	2.85×10^{8},	1.14×10^{7},	1.00×10^{7},	1.80×10^{2},	-	2.32×10^{11},	3.27×10^{6},	1.60×10^{3},
215.6	10	2.13×10^{-11},	1.47×10^{-15},	2.19×10^{-17},	4.48×10^{-15},	7.06×10^{-21},	1.09×10^{-24},	7.28×10^{-11},	9.00×10^{-17},	7.11×10^{-21},
		7.25×10^{8},	5.01×10^{4},	7.48×10^{2},	1.31×10^{5},	-	-	2.48×10^{9},	3.06×10^{3},	-
8.0	15	9.04×10^{-14},	1.68×10^{-18},	9.14×10^{-21},	1.50×10^{-16},	3.44×10^{-23},	1.17×10^{-27},	1.93×10^{-12},	1.41×10^{-19},	5.89×10^{-24},
		3.35×10^{6},	6.26×10^{1},	-	5.12×10^{3},	-	-	7.18×10^{7},	1.29×10^{1},	-
208.0	20	5.28×10^{-15},	1.10×10^{-20},	5.39×10^{-24},	1.67×10^{-17},	5.91×10^{-25},	2.44×10^{-30},	2.57×10^{-13},	2.46×10^{-20},	1.48×10^{-26},
		1.87×10^{5},	-	-	6.22×10^{2},	-	-	9.08×10^{6},	-	-
216.0	25	1.37×10^{-15},	8.30×10^{-22},	9.91×10^{-26},	3.80×10^{-18},	4.91×10^{-26},	6.18×10^{-32},	6.99×10^{-14},	7.07×10^{-22},	4.53×10^{-28},
		4.68×10^{4},	-	-	1.34×10^{2},	-	-	2.37×10^{6},	-	-
221.5	30	4.65×10^{-16},	1.13×10^{-22},	4.97×10^{-27},	8.40×10^{-19},	5.11×10^{-27},	2.71×10^{-33},	2.11×10^{-14},	1.00×10^{-22},	2.74×10^{-29},
		1.54×10^{4},	-	-	2.86×10,	-	-	7.01×10^{5},	-	-
228.1	35	1.27×10^{-16},	1.08×10^{-23},	1.45×10^{-28},	1.32×10^{-19},	3.30×10^{-28},	6.32×10^{-35},	5.80×10^{-15},	1.13×10^{-23},	1.12×10^{-30},
		4.11×10^{3},	-	-	-	-	-	1.87×10^{5},	-	-
240.5	40	2.78×10^{-17},	5.33×10^{-25},	1.32×10^{-30},	1.82×10^{-20},	1.40×10^{-29},	6.55×10^{-37},	1.48×10^{-15},	8.92×10^{-25},	2.18×10^{-32},
		8.50×10^{2},	-	-	-	-	-	4.54×10^{4},	-	-
251.9	45	5.57×10^{-18},	2.61×10^{-26},	1.34×10^{-32},	1.97×10^{-21},	4.78×10^{-31},	5.84×10^{-39},	3.58×10^{-26},	6.78×10^{-26},	4.38×10^{-34},
		1.62×10^{2}	-	-	-	-	-	1.04×10^{4}	-	-

0.031; FWHM value of 60 cm^{-1} K_p = 0.040 and FWHM value of 100 cm^{-1} K_p = 0.055; note a K_p value of 0.055 was considered to be an upper limit). Note the corresponding water dimer number densities, $N_{H_2O{\cdot}H_2O}$, for FWHM values of 40, 60, and 100 cm^{-1} are 2.2×10^{14} cm^{-3}, 2.8×10^{14} cm^{-3}, and 3.9×10^{14} cm^{-3}, respectively. Clearly, the relatively broad range of values reported for the dimer band FWHM and uncertainties due to the large noise to signal ratio make it difficult to determine an accurate value for the dimerization equilibrium constant. It is nevertheless remarkable that the range of K_p values obtained from DOAS measurements by *Lotter* [2006] reasonably agree with the extrapolated K_p values by *Curtiss et al.* [1979] and our quantum chemical calculations (see Figure 2). For instance, our CBS-Q values for K_p and $N_{H_2O{\cdot}H_2O}$ obtained at the same temperature, i.e., 301 K, are 0.043 and 3.0×10^{14} cm^{-3} (0.074% of total water), respectively, and are in good agreement with the data reported by *Lotter* [2006]. Results from G3 calculations at 301 K yield values for K_p and $N_{H_2O{\cdot}H_2O}$ of 0.033 and 2.3×10^{14} cm^{-3}, respectively, which, in turn, lends support to the accuracy of CBS-Q and G3 type of calculations on water clusters. However, so far, the results by *Lotter* [2006] represent the only experimental determinations of water clustering equilibria at atmospheric conditions. Unfortunately, there are no reported measurements concerning the abundance of higher water clusters and clusters of the $N_2O{\cdot}(H_2O)_n$ and $CO_2{\cdot}(H_2O)_n$ series in atmospheric media.

[25] One of the more important points illustrated in Table 5 is the high abundance of $N_2O{\cdot}H_2O$ and $CO_2{\cdot}H_2O$ clusters predicted to be present in the atmosphere up to 45 km as well as significant levels of higher hydrates in the lower troposphere (i.e., $\leq$10 km altitude). At a temperature of 298 K, our CBS-Q calculations predict number densities for $N_2O{\cdot}(H_2O)$ and $CO_2{\cdot}(H_2O)$ in the range of 2.7×10^8 cm^{-3} and 9.5×10^{11} cm^{-3}, which corresponds to a ratio of monomer (i.e., unhydrated N_2O or CO_2) to monohydrate of around 29,000 and 10,000, respectively. Thus, it is probable that in addition to the $H_2O{\cdot}(H_2O)$ moiety, other clusters, such as, for instance, the $CO_2{\cdot}(H_2O)$ cluster could be present in sufficient quantities to have a nontrivial effect on solar absorption.

[26] Another noticeable point in Table 5 is the predicted high abundance of larger $H_2O{\cdot}(H_2O)_n$ clusters within the troposphere. For example, at sea level, where the water monomer number density is around 4.2×10^{17} cm^{-3}, the number densities of $H_2O{\cdot}(H_2O)$, $H_2O{\cdot}(H_2O)_2$, $H_2O{\cdot}(H_2O)_3$ are 1.9×10^{14} cm^{-3} (or 7.6×10^{-6} atm), 1.3×10^{11} cm^{-3} (5.4×10^{-9} atm), 6.8×10^{9} cm^{-3} (2.8×10^{-10} atm), respectively. Using a standard statistical thermodynamic approach, *Headrick and Vaida* [2001] have calculated altitude profiles (35 km) for water clusters up to the tetramer and, more interestingly, provided an outlook on how individual clustering equilibria are affected by temperature increases in a simulated global warming scenario (i.e., a uniform 2 K increase up to 35 km altitude). As expected, abundances of clusters with higher water numbers decreased with increasing altitude. However, every $H_2O{\cdot}(H_2O)_n$ profile displayed a comprehensive nonlinear increase in abundance when temperature was increased and solar absorption was predicted to shift up by 0.05 W m^{-2} to values of around 0.5 W m^{-2}. It should be noted that such elevated levels of atmospheric water oligomers are also anticipated

to have a significant effect on the catalysis of atmospheric reactions. For instance, in the case of carbon dioxide hydration increasing toward carbonic acid, it has been demonstrated that a three-membered water cluster ring plays an essential role in the hydration reaction of CO_2 where the $CO_2 \cdot (H_2O)_3$ transition cluster is oriented in an optimal manner to promote proton transfer in a rapid and concerted step [*Nguyen et al.*, 1997]. Interestingly, similar water clustering reactions might proceed around other atmospheric gases such as formic acid [*Aloisio et al.*, 2002], acetic acid [*Khare et al.*, 1999], and potentially other small biomolecules, such as, for instance, neutral and zwitter-ionic glycine, which form strong hydrogen bonds, such that hydrated clusters would form a significant atmospheric repository of these species.

[27] **Acknowledgments.** The authors want to thank O. Suleimenov (ETH-Zürich) for valuable discussions about cluster structure optimization. We also wish to thank T.K. Ha (ETH-Zürich) for fruitful discussions on ab initio theory and its application to solving thermochemical problems. The Competence Centre for Computational Chemistry (C4) at ETH-Zürich is also thanked for providing access and support to its facilities. Finally, two anonymous reviewers and Associate Editor J. Fuentes are thanked for their constructive comments on the manuscript. This work was carried out at the Swiss Federal Institute of Technology (ETH), Zürich, and funded by Schweizerischer Nationalfonds grant 200020–113476 awarded to T.M. Seward.

References

Aloisio, S., P. E. Hintze, and V. Vaida (2002), The hydration of formic acid, *J. Phys. Chem. A*, *106*, 363–370, doi:10.1021/jp012190l.

Brasseur, G. P., and S. Solomon (2005), *Aeronomy of the Middle Atmosphere: Chemistry and Physics of the Stratosphere and Mesosphere*, 3rd ed., 646 pp., Springer, New York.

Coan, C. R., and A. D. King (1971), Solubility of water in compressed carbon dioxide, nitrous oxide and ethane - evidence for hydration of carbon dioxide and nitrous oxide in the gas phase, *J. Am. Chem. Soc.*, *93*, 1857–1862, doi:10.1021/ja00737a004.

Cox, A. J., T. A. Ford, and L. Glasser (1994), Ab *initio* molecular orbital calculations of the infrared spectra of interacting water molecules. IV: Interaction energies and band intensities of the complexes of water with carbon dioxide and nitrous oxide, *J. Mol. Struct. THEOCHEM*, *312*, 101–108.

Cruzan, J. D., L. B. Braly, K. Liu, M. G. Brown, J. G. Loeser, and R. J. Saykally (1996), Quantifying hydrogen bond cooperativity in water: VRT spectroscopy of the water tetramer, *Science*, *271*, 59–62, doi:10.1126/science.271.5245.59.

Curtiss, L. A., D. J. Frurip, and M. Blander (1978), A study of dimerization in water vapor by measurement of thermal conductivity, *Chem. Phys. Lett.*, *54*, 575–578, doi:10.1016/0009-2614(78)85290-7.

Curtiss, L. A., D. J. Frurip, and M. Blander (1979), Studies of molecular association in H_2O and D_2O vapors by measurement of thermal conductivity, *J. Chem. Phys.*, *71*, 2703–2727, doi:10.1063/1.438628.

Curtiss, L. A., K. Raghavachari, P. C. Redfern, V. Rassolov, and J. A. Pople (1998), Gaussian-3 theory for molecular energies of first- and second-row compound, *J. Chem. Phys.*, *109*, 7764–7776, doi:10.1063/1.477422.

Curtiss, L. A., K. Raghavachari, P. C. Redfern, and J. A. Pople (2000), Assessment of Gaussian-3 and density functional theories for a larger test set, L. A., *J. Chem. Phys.*, *112*, 7374–7383, doi:10.1063/1.481336.

Day, M. B., K. N. Kirschner, and G. C. Shields (2005), Global search for minimum energy $(H_2O)_n$ clusters, n = 3–5, *J. Phys. Chem. A*, *109*, 6773–6778, doi:10.1021/jp0513317.

Diri, K., E. M. Myshakin, and K. D. Jordan (2005), On the contribution of vibrational anharmonicity to the binding energies of water clusters, *J. Phys. Chem. A*, *109*, 4005–4009, doi:10.1021/jp050004w.

Dunn, M. E., E. K. Pokon, and G. C. Shields (2004), Thermodynamics of forming water clusters at various temperatures and pressures by gaussian-2, gaussian-3, complete basis set-QB3, and complete basis Set-APNO model chemistries; Implications for atmospheric chemistry, *J. Am. Chem. Soc.*, *126*, 2647–2653, doi:10.1021/ja038928p.

Dunning, T. H. (2000), A road map for the calculation of molecular binding energies, *J. Phys. Chem. A*, *104*, 9062–9080, doi:10.1021/jp001507z.

Dyke, T. R., and J. S. Muentner (1974), Microwave spectrum and structure of hydrogen bonded water dimer, *J. Chem. Phys.*, *60*, 2929–2930, doi:10.1063/1.1681463.

Fellers, R. S., C. Leforestier, L. B. Braly, M. G. Brown, and R. J. Saykally (1999), Spectroscopic determination the water pair potential, *Science*, *284*, 945–948, doi:10.1126/science.284.5416.945.

Frisch, M. J., et al. (2003), *GAUSSIAN03, Revision C.02*, Gaussian Inc., Pittsburgh, Pa.

Gebbie, H. A., W. J. Burroughs, J. Chamberlain, J. E. Harries, and R. G. Jones (1969), Dimers of the water molecule in the Earth's atmosphere, *Nature*, *221*, 143–145, doi:10.1038/221143a0.

Gimmler, G., and M. Havenith (2002), High-resolution IR spectroscopy of the N_2O-H_2O and N_2O-D_2O van der Waals complexes, *J. Mol. Spectrosc.*, *216*, 315–321, doi:10.1006/jmsp.2002.8687.

Goldman, N., R. S. Fellers, C. Leforestier, and R. J. Saykally (2001), Water dimers in the atmosphere: equilibrium constant for water dimerization from the VRT (ASP-W) potential surface, *J. Phys. Chem. A*, *105*, 515–519, doi:10.1021/jp003567a.

Headrick, J. E., and V. Vaida (2001), Significance of water complexes in the atmosphere, *Phys. Chem. Earth C*, *26*, 479–486.

Jena, N. R., and P. C. Mishra (2005), An *ab initio* and density functional study of microsolvation of carbon dioxide in water clusters and formation of carbonic acid, *Theor. Chem. Acc.*, *114*, 189–199, doi:10.1007/s00214-005-0660-1.

Keutsch, F. N., and R. J. Saykally (2001), Water clusters: Untangling the mysteries of the liquid, one molecule at a time, *Proc. Natl. Acad. Sci. U. S. A.*, *98*, 10,533–10,540, doi:10.1073/pnas.191266498.

Khare, P., N. Kumar, K. M. Kumari, and S. S. Srivastava (1999), Atmospheric formic and acetic acids: An overview, *Rev. Geophys.*, *37*, 227–248, doi:10.1029/1998RG900005.

Kjaergaard, H. G., T. W. Robinson, D. L. Howard, J. S. Daniel, J. E. Headrick, and V. Vaida (2003), Complexes of importance to the absorption of solar radiation, *J. Phys. Chem. A*, *107*, 10,680–10,686, doi:10.1021/jp035098t.

Likholyot, A., K. H. Lemke, J. K. Hovey, and T. M. Seward (2007), Mass spectrometric and quantum chemical determination of proton-water-clustering equilibria, *Geochim. Cosmochim. Acta*, *71*, 2436–2447, doi:10.1016/j.gca.2007.02.022.

Linstrom, P. J., and W. G. Mallard (Eds.) (2005), *NIST Chemistry WebBook, NIST Standard Reference Database Number 69*, Natl. Inst. of Stand. and Technol., Gaithersburg, Md. (Available at http://webbook.nist.gov)

Liu, K., J. G. Loeser, M. J. Elrod, B. C. Host, J. A. Rzepiela, N. Pugliano, and R. J. Saykally (1994), Dynamics of structural rearrangements in the water trimer, *J. Am. Chem. Soc.*, *116*, 3507–3512, doi:10.1021/ja00087a042.

Liu, K., J. D. Cruzan, and R. J. Saykally (1996), Water clusters, *Science*, *271*, 929–933, doi:10.1126/science.271.5251.929.

Liu, K., M. G. Brown, and R. J. Saykally (1997a), Terahertz laser vibration-rotation tunneling spectroscopy and dipole moment of a cage form of the water hexamer, *J. Phys. Chem. A*, *101*, 8995–9010, doi:10.1021/jp9707807.

Liu, K., M. G. Brown, J. D. Cruzan, and R. J. Saykally (1997b), Terahertz laser spectroscopy of the water pentamer: Structure and hydrogen bond rearrangement dynamics, *J. Phys. Chem. A*, *101*, 9011–9021, doi:10.1021/jp970781z.

Lotter, A. (2006), Field measurements of water continuum and water dimer absorption by active long path differential optical absorption spectroscopy (DOAS), Ph.D. thesis, 173 pp., Univ. of Heidelberg, Germany, 5 July.

Masamura, M. (2001), The effect of basis set superposition error on the convergence of interaction energies, *Theor. Chem. Acc.*, *106*, 301–313, doi:10.1007/s002140100280.

Montgomery, J. A., J. W. Ochterski, and G. A. Petersson (1994), A complete basis set model chemistry. IV. An improved atomic pair natural orbital method, *J. Chem. Phys.*, *101*, 5900–5909, doi:10.1063/1.467306.

Nguyen, M. T., and T. K. Ha (1984), Theoretical study of the formation of carbonic acid from the hydration of carbon dioxide: A case of active solvent catalysis, *J. Am. Chem. Soc.*, *106*, 599–602, doi:10.1021/ja00315a023.

Nguyen, M. T., G. Raspoet, L. G. Vanquickenborne, and P. T. Van Duijnen (1997), How many water molecules are actively involved in the neutral hydration of carbon dioxide?, *J. Phys. Chem. A*, *101*, 7379–7388, doi:10.1021/jp9701045.

Ochterski, J. W., G. A. Petersson, and J. A. Montgomery (1996), A complete basis set model chemistry. V. Extensions to six or more heavy atoms, *J. Chem. Phys.*, *104*, 2598–2619, doi:10.1063/1.470985.

Peterson, K. I., and W. Klemperer (1984), Structure and internal rotation of H_2O-CO_2, HDO-CO_2, and D_2O-CO_2 van der Waals complexes, *J. Chem. Phys.*, *80*, 2439–2445, doi:10.1063/1.446993.

Peterson, K. I., R. D. Suenram, and F. J. Lovas (1991), Hydration of carbon dioxide: The structure of H_2O-H_2O-CO_2 from microwave spectroscopy, *J. Chem. Phys.*, *94*, 106–117, doi:10.1063/1.460384.

Pfeilsticker, K., A. Lotter, C. Peters, and H. Bosch (2003), Atmospheric detection of water dimers via near-infrared absorption, *Science*, *300*, 2078–2080, doi:10.1126/science.1082282.

Ptashnik, I. V., K. M. Smith, K. P. Shine, and D. A. Newnham (2004), Laboratory measurements of water vapour continuum absorption in spectral region 5000–5600 cm-1: Evidence for water dimers, *Q. J. R. Meteorol. Soc.*, *130*, 2391–2408, doi:10.1256/qj.03.178.

Pugliano, N., and R. J. Saykally (1992), Measurement of quantum tunneling between chiral isomers of the cyclic water trimer, *Science*, *257*, 1937–1940.

Scribano, Y., N. Goldman, R. J. Saykally, and C. Leforestier (2006), Water dimers in the atmosphere III: Equilibrium constant from a flexible potential, *J. Phys. Chem. A*, *110*, 5411–5419, doi:10.1021/jp056759k.

Slanina, Z. (1988), A theoretical evaluation of water oligomer populations in the Earth's atmosphere, *J. Atmos. Chem.*, *6*, 185–190, doi:10.1007/BF00053854.

Slanina, Z., F. Uhlik, A. T. Saito, and E. Osawa (2001), Computing molecular complexes in Earth's and other atmospheres, *Phys. Chem. Earth, Part C*, *26*, 505–511.

Slanina, Z., H. Uhlik, S. L. Lee, and S. Nagase (2006), Computational modelling for the clustering degree in the saturated steam and the water-containing complexes in the atmosphere, *J. Quant. Spectrosc. Radiat. Transfer.*, *97*, 415–423, doi:10.1016/j.jqsrt.2005.05.065.

Vaida, V., J. S. Daniel, H. G. Kjaergaard, L. Goss, and A. F. Tuck (2001), Atmospheric absorption of near infrared and visible solar radiation by the hydrogen bonded water dimer, *Q. J. R. Meteorol. Soc.*, *127*, 1627–1643.

Vaida, V., H. G. Kjaergaard, and K. J. Feierabend (2003), Hydrated complexes: relevance to atmospheric chemistry and climate, *Int. Rev. Phys. Chem.*, *22*, 203–219, doi:10.1080/0144235031000075780.

Wójcik, M. J., M. Boczar, and T. A. Ford (2001), Ab initio study of energies, structures and vibrational spectra of the complexes of water with carbon oxysulfide and nitrous oxide, *Chem. Phys. Lett.*, *348*, 126–130, doi:10.1016/S0009-2614(01)01056-9.

Zolandz, D., D. Yaron, K. I. Peterson, and W. Klemperer (1992), Water in weak interactions: the structure of the water-nitrous oxide complex, *J. Chem. Phys.*, *97*, 2861–2868, doi:10.1063/1.463028.

K. H. Lemke, Department of Earth Sciences, University of Hong Kong, James H. Lee Science Building, Pofkulam Road, Hong Kong. (kono@hku.hk)

T. M. Seward, Institute of Mineralogy and Petrology, ETH Zurich, CH-8092 Zurich, Switzerland.